

# Electronic structure and light-induced conductivity in a transparent refractory oxide

J. E. Medvedeva<sup>1,\*</sup>, A. J. Freeman<sup>1</sup>, M. I. Bertoni<sup>2</sup> and T. O. Mason<sup>2</sup>

<sup>1</sup>*Department of Physics and Astronomy and* <sup>2</sup>*Department of Materials Science and Engineering, Northwestern University, Evanston, Illinois 60208-3112*

Combined first-principles and experimental investigations reveal the underlying mechanism responsible for a drastic change of the conductivity (by 10 orders of magnitude) following hydrogen annealing and UV-irradiation in a transparent oxide,  $12\text{CaO}\cdot 7\text{Al}_2\text{O}_3$ , found by Hayashi *et al.* The charge transport associated with photo-excitation of an electron from H, occurs by electron hopping. We identify the atoms participating in the hops, determine the exact paths for the carrier migration, estimate the temperature behavior of the hopping transport and predict a way to enhance the conductivity by specific doping.

PACS numbers: 71.20.-b, 72.20.Ee, 72.40.+w, 81.05.Je

The rare combination of transparency and conductivity has a wide range of technological applications<sup>1</sup>. Until recently, optimum optical transmission and useful electrical conductivity ( $>10^3 \text{ S cm}^{-1}$ ) was attained by the introduction of selected dopants into a wide-bandgap oxide. Hence the excitement surrounding the report that Hayashi *et al* found a new way to convert a transparent oxide into a persistent electronic conductor<sup>2</sup> with the potential for less expensive and more flexible optoelectronic devices (including flat panel displays, solar cells, invisible circuits) as well as three-dimensional holographic memories. Despite careful experimental studies, no definitive understanding has been reached on the underlying mechanism responsible for this new dramatic effect. In this combined theoretical and experimental investigation, we address the nature of this novel phenomenon which is crucial for further progress and make predictions on how to improve the conductivity toward the level where it becomes useful for practical applications.

We have reproduced in bulk form the single crystal and thin film results of Hayashi *et al* by solid state reaction of high purity oxides<sup>3</sup> (99.99+%), followed by hydrogen treatment (5% $\text{H}_2$ /95% $\text{N}_2$ ) of sintered pellets at 1,300 °C for 2 h, and by quenching to room temperature. UV-treatment was performed under a mercury arc lamp (40 min at 20  $\text{mW cm}^{-2}$  and a wavelength of 220 nm). This turned a surface layer of  $\sim 16 \mu\text{m}$  thickness from white to green, with a conductivity changed from  $10^{-10}$  to  $0.6 \text{ S cm}^{-1}$  (by four-point method). We also irradiated loose H-treated powders, which also turned from white to a uniform green color, and measured their conductivity by a “powder-solution-composite” method<sup>4</sup> to be  $0.41 \text{ S cm}^{-1}$ . Both values agree with those in Ref. 2 and provide confidence in our experimental confirmation of the predictions reported below.

From the theoretical side, we demonstrate with density functional calculations that the conductivity appears to result from electrons excited off the hydrogen ions into conduction bands formed from Ca 3d states. The changes found in the electronic properties caused by the UV-irradiation of H-doped mayenite allow us to conclude that the observed absorption peak at 0.4 eV has a fundamentally different nature than the  $\text{F}^+$  center energy

level originally assumed in Ref. 2 and followed in recent theoretical work<sup>5</sup>. Our calculated charge density shows clearly that electron trapping on a vacancy (i.e., formation of the  $\text{F}^+$  center) does not occur in the case of UV-irradiated H-doped mayenite. Instead, we identify the atoms participating in hopping transport; estimates of the characteristic parameters that determine the behavior of the hopping conductivity at low (Efros-Shklovskii regime) and high (Mott) temperatures agree reasonably well with experiment. Finally, we found a strong dependence of the electronic transport on the particular hopping centers and their spatial arrangement that allows the prediction of rates of temperature treatment and dopants which will enhance the conductivity.

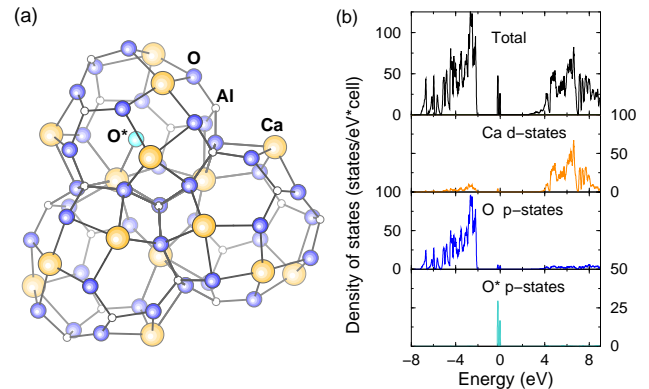


FIG. 1. (a) Three of the 12 cages constituting a unit cell of mayenite. An  $\text{O}^{2-}$  anion (abbreviated as  $\text{O}^*$ ) is located inside one of six cages so that the distances between  $\text{O}^*$  and its six neighbor Ca atoms vary from 2.36 to 3.95 Å. (b) Total and partial DOS of  $12\text{CaO}\cdot 7\text{Al}_2\text{O}_3$ ;  $E_F$  is at 0 eV. The Al 3d states form the band centered at  $\sim 28$  eV.

The crystal structure of  $12\text{CaO}\cdot 7\text{Al}_2\text{O}_3$  has the space group  $I\bar{4}3d$ , with two formula units in the unit cell and a lattice parameter of 11.98 Å (Ref. 6, 7). This framework includes 64 of the oxygen atoms; the remaining two oxygen ions (abbreviated as  $\text{O}^*$  hereafter) which provide charge neutrality<sup>7</sup> are located inside the cages, Fig. 1(a). These two  $\text{O}^*$  are distributed between 24 sites that produce a structural disorder. From full-potential linearized

augmented plane-wave<sup>8</sup> (FLAPW) total energy calculations of seven structures with different distances between these two oxygen ions (ranging from 5.1 Å to 10.4 Å), we found that the O\*s tend to maximize the distance between them by forming a bcc lattice with the crystallographic basis oriented randomly with respect to that of the whole crystal. After hydrogen annealing, changes in the crystal structure are not observed<sup>9</sup>. The incorporation of H<sup>-</sup> ions corresponds to the following chemical reaction: O<sup>2-</sup> (cage) + H<sub>2</sub> (atm.) → OH<sup>-</sup> (cage) + H<sup>-</sup> (in another cage), so the unit cell contains two cages occupied by O\*H, another two by hydrogen ions (abbreviated as H\* hereafter) and the remaining 8 cages are empty<sup>10</sup>. From the electronic structure calculations, we found that the structure with two H<sup>-</sup> ions in cages and released O<sub>2</sub> gas (cf., Ref. 2) leads to an insulating state after photo-activation.

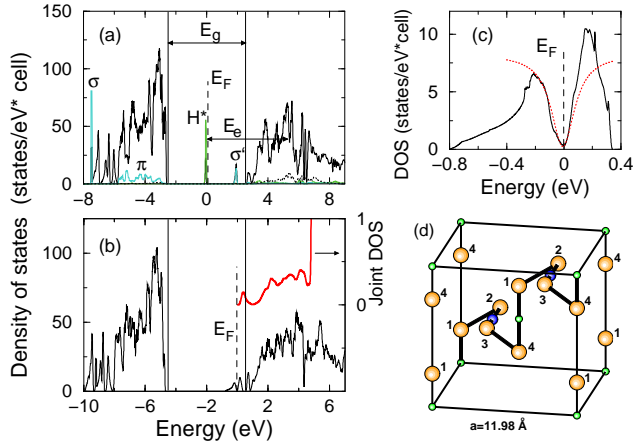


FIG. 2. (a) Total DOS of H-bearing mayenite. The band gap,  $E_g$ , is between O 2p and Ca 3d states. The DOS of the impurity bands arising from the OH<sup>-</sup> complex and H\* is enlarged by a factor of five. The photo-activation of the H\* corresponds to the transition from H\* 1s states to the 3d states of its closest Ca (dashed line), with energy  $E_e$ . (b) Total DOS of UV-irradiated H-doped mayenite and the joint DOS (thick line) calculated using the optical selection rules and only nearest neighbor transitions which have higher probability. (c) Enlarged total DOS of UV-irradiated H-doped mayenite and a theoretical fit to the DOS near  $E_F$  (dashed line), see text. (d) The optimal path for electron migration throughout the crystal. The cube represents a full unit cell consisting of 12 cages (118 atoms); only atoms which give the dominant contribution to the band crossing  $E_F$  are shown – Ca (largest spheres), O\* (between Ca(2) and Ca(3)) and H\* (smallest spheres).

The calculated<sup>11</sup> electronic density of states (DOS) before H-doping is shown in Fig. 1(b): oxygen 2p states form the top of the valence band between -6 eV and -2 eV (the Fermi level is taken as zero), while the bottom of the conduction band is formed from Ca 3d states. Located inside one of the six cages, O\* gives a fully occupied impurity peak below  $E_F$ . The calculated band gap, 4.8

eV, underestimates the experimental absorption edge<sup>2</sup> by 4%. The incorporation of H ions into the cages of insulating mayenite results in the appearance of new bands (Fig. 2(a)): (i) since H shares its electron with O\* (and forms an OH<sup>-</sup> complex), filled  $\sigma$  and non-bonding  $\pi$  bands and unoccupied  $\sigma'$  band are introduced; and (ii) the 1s states of H\* form the fully occupied impurity band below  $E_F$ . After the H-doping, the energy of the transitions from O 2p states to Ca 3d states is decreased by 0.7 eV (from 5.9 eV to 5.2 eV), in agreement with experiment<sup>2</sup>. The maximum efficiency of the photo-activation of the H\*, which corresponds to transitions from H\* 1s states to the 3d states of its closest Ca neighbors, occurs at about the same photon energy (Fig. 2(a)). These results are in contrast with the conclusion of Ref. 2 that hydrogen controls the absorption edge.

For UV-irradiated H-bearing mayenite, the electron excitation from H\* is calculated with the model system where the electron is transferred equally to the d states of six Ca neighbors<sup>12</sup>. The self-consistent DOS shows the formation of a new band (Fig. 2(b)) with the same total number of states,  $m$ , as in the band gap of the system before UV irradiation. However, since  $m$  is now two times larger than the number of available electrons,  $E_F$  passes through the middle of the band and the system becomes conducting. The calculated positions of the characteristic absorption bands (0.38 eV and 3.5 eV, Fig. 2(b)) are in good agreement with experiment (0.4 eV and 2.8 eV), as is the intense charge transfer transition from oxygen 2p states to Ca 3d states which occurs at  $\sim 4.8$  eV.

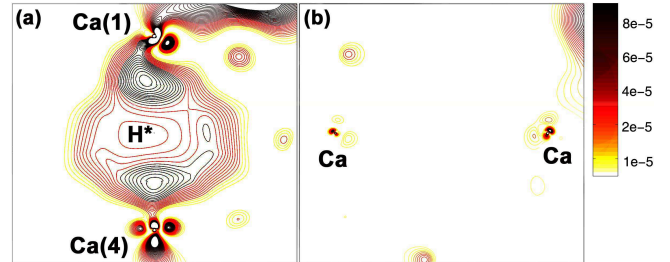


FIG. 3. Contour map of the charge density distribution within a slice passing through the center of (a) a cage with H\* and (b) an empty one (vacancy).

As shown in Fig. 2(c), the non-zero DOS at  $E_F$ ,  $g(E_F)$ , is determined mainly by H\*, O\* and Ca states – atoms that are spatially well separated from each other (Fig. 2(d)), which points to the hopping nature of the induced conductivity. It is striking that the arrangement of the atoms corresponds to the shortest electron hopping path: only the closest Ca neighbors of O\*, Ca(2) and Ca(3) (at distances of 3.3 and 2.4 Å, respectively), and the closest Ca neighbors of H\*, Ca(1) and Ca(4) (both at 2.8 Å), give significant contributions to  $g(E_F)$  (Table I). The longest segment on the hopping path corresponds to the distance between Ca(1), Ca(2) and O\*, which explains the higher probability to find the electron on Ca(1) and Ca(2). Finally, the charge density distribution calculated

in the energy window of 25 meV below  $E_F$ , clearly shows the connected electron density maxima along the hopping path (cf., Fig. 3(a)). The charge density in the empty cages is insignificant (cf., Fig. 3(b)), demonstrating that trapping of the electron on the vacancy does not occur<sup>13</sup>.

Hopping transport in systems with localized electronic states has been studied analytically, numerically and experimentally<sup>14–16</sup>. At high temperatures (T) the hopping occurs between nearest neighbors and has an activated nature. At lower T, the activation energy for hops between localized centers can be reduced by enlarging the hopping distance – which leads to the variable-range hopping described by Mott<sup>14</sup>. At yet lower T, the electron-electron repulsive interaction between charge carriers may result in the formation of a Coulomb gap centered at  $E_F$ . The DOS at  $E_F$  may not turn exactly to zero, corresponding to a ‘soft’ Coulomb gap<sup>15</sup>: this residual DOS at  $E_F$  is caused by correlated simultaneous hops of several electrons (multi-electron hopping) which plays a dominant role<sup>17</sup> at extremely low T.

Similar to the above qualitative picture, we predict the behavior of the conductivity at finite T based on the calculated DOS in the vicinity of  $E_F$  for the irradiated H-doped mayenite. Clearly, this exhibits in Fig. 2(c) a soft Coulomb gap near  $E_F$  and, similar to Fig. 10.1 in Ref. 15, has two peaks. These results conform to the Efros-Shklovskii (ES) behavior<sup>15</sup> of the conductivity  $\sigma$  at low T:

$$\sigma = \sigma_0 \exp[-(T_{ES}/T)^{1/2}], \quad T_{ES} = \beta_{ES} e^2 / k_B k \xi, \quad (1)$$

where  $\xi$  is the localization length,  $e$  – the elementary charge,  $k_B$  – the Boltzmann constant, and  $k = \epsilon_0 \epsilon_r$  is the dielectric constant ( $\epsilon_0$  – the permittivity constant and  $\epsilon_r$  – the relative dielectric constant). When T increases, the Coulomb gap fills. According to Ref. 18, a substantial DOS should be observed already at  $T \sim 0.05 \Delta \epsilon$ , where  $\Delta \epsilon$  is the gap width. At this T, the changeover to the Mott behavior<sup>14</sup> should occur:

$$\sigma = \sigma_0 \exp[-(T_M/T)^{1/4}], \quad T_M = \beta_M / k_B g_0 \xi^3. \quad (2)$$

The double peak structure completely disappears at  $T \sim 0.4 \Delta \epsilon$ . Using  $\Delta \epsilon \simeq 0.3$  eV (Fig. 2(c)), we obtain the crossover temperature between Mott and ES behavior to be  $T_c \simeq 170$  K. Indeed, for H-doped UV-irradiated mayenite, the  $T^{-1/4}$  dependence of  $\log(\sigma)$  was found experimentally<sup>2</sup> for  $50 < T < 300$  K. Further, the calculated DOS near  $E_F$  fits well (Fig. 2(c)) with the theoretical one of the form  $g(E) = \alpha E_c^2 E^2 / (E_c^2 + E^2)$ , where  $\alpha = (3/\pi)(k^3/e^6)$ . In the high energy limit, the DOS has the constant value of  $g_0 \equiv \alpha E_c^2$  that corresponds to Mott behavior. In the opposite limit, it approaches a parabolic dependence (ES) which has only one physical parameter – the refractive index,  $n$ . We found  $n \simeq 2.1$ , while the experiment<sup>20</sup> gives  $n = 1.6$ . From the fit, we obtain  $g_0 \simeq 8$  states/eV-cell and  $\alpha \simeq 800$  which allows us to estimate

the characteristic T: using  $\beta_M = 7.6$  (Ref. 19),  $\beta_{ES} = 2.8$  (Ref. 15) and the localization length  $\xi = 1.5$  Å (which is comparable to the ionic radii of the atoms involved in the hops), we obtain  $T_M \simeq 5.6 \times 10^6$  K which agrees fairly well with the experimental value<sup>2</sup>,  $T_M = 2 \times 10^6$  K, and predict that  $T_{ES} \simeq 2.7 \times 10^4$  K. Thus, our band structure calculations give reasonable order of magnitude estimates for the characteristic T of the hopping transport in mayenite. Of course, more precise determinations require temperature and time-dependent calculations.

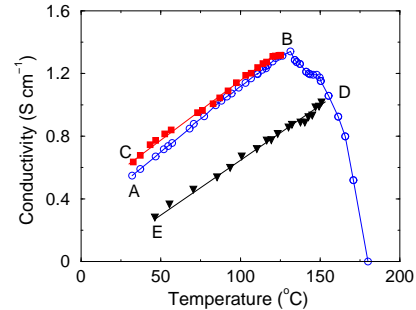


FIG. 4. Measured  $\sigma$ -T characteristics of the UV-irradiated H-doped  $12\text{CaO} \cdot 7\text{Al}_2\text{O}_3$  bulk samples of 46% density. Due to the realization of the optimal arrangement of the hopping centers during the heat treatment (A→B), the conductivity is enhanced after cooling the sample (B→C). Subsequent T cycling (B↔C) does not result in any changes of  $\sigma$ , i.e., the system is reversible. Cooling from any point above the conductivity maximum, as in path (D→E), shows reduced  $\sigma$  unchanged by UV irradiation at room T (E↔D), as expected from the release of H.

Since  $\text{H}^*$  may also occupy cages located farther away from the one with an  $\text{O}^*\text{H}$ , we investigated this arrangement and found it to be less favorable energetically – by 96 meV. However, under the rapid cooling of the sample annealed at  $1,300$  °C some  $\text{H}^*$  can become “frozen” into these positions. After UV irradiation, the corresponding hopping path involves a very long segment between two Ca atoms (now increased from 3.7 to 6.5 Å), so that the DOS at  $E_F$  becomes zero and the hopping has an activated behavior. If now T is increased to a level sufficient for hydrogen migration, these  $\text{H}^*$  will be able to diffuse into the energetically favorable positions which facilitates the hopping and leads to an increase of the conductivity. We confirmed these predictions experimentally, as shown in Fig. 4. Moreover, our samples showed non-reversible behavior once T is increased above  $T_m$ , the conductivity maximum: the decay of the conductivity is associated with hydrogen release from the sample which breaks up the hopping path.

If one focusses on the strong dependence of the photo-induced conductivity on the particular atoms participating in the hopping and their spatial arrangement, one is able to predict the possibility of varying the conductivity by proper doping. For example, we expect that Mg substitution can lead to a decrease in the conductivity once Mg substitutes one of the Ca atoms involved in the hop-

ping, since its 3d states will lie much higher in energy than that of Ca, while Sr substitution may not result in any significant changes in the conductivity. Instead, one way to possibly improve the electronic transport of the material consists in increasing the concentration of hopping centers. For this, the poorly bonded  $O^{2-}$  ion inside a cage of mayenite, is easily replaced by  $2F^-$  or  $2Cl^-$  ions that will allow some enhancement of the conductivity since the number of hopping centers and the number of carriers is now doubled. Recent observations agree with our model and its predictions: proton implantation was found to increase the conductivity as compared with thermal H-treatment<sup>21</sup>. Our additional calculations show that along with the increased concentration of the encaged electrons, the proton implantation will result in the appearance of new unoccupied states in the band gap making  $H^+$  one of the hopping centers that creates a conductivity channel and so enhances the transport.

Finally, the encouraging findings obtained in this first *ab-initio* study of hopping transport suggest that important results may also be obtained when a similar approach is applied to such systems as doped semiconductors, manganite perovskites, carbon nanotubes, etc<sup>22</sup>.

We thank V.P. Dravid for sharing his unpublished electron microscopy results. Work supported by the DOE (grant N DE-FG02-88ER45372) and the NSF through its MRSEC program at the Northwestern Materials Research Center. Computational resources have been provided by the DOE supported NERSC.

\* Corresponding author.

Email address: j-medvedeva@northwestern.edu

- 
- <sup>1</sup> G. Thomas, Nature **398**, 907 (1997); D. S. Ginley, and C. Bright, MRS Bull. **25**, 15 (2000); B. G. Lewis, and D. C. Paine, MRS Bull. **25**, 22 (2000); H. Kawazoe, H. Yanagi, K. Ueda, and H. Hosono, MRS Bull. **25**, 28 (2000).  
<sup>2</sup> K. Hayashi, S. Matsuishi, T. Kamiya, M. Hirano, and H. Hosono, Nature **419**, 462 (2002).  
<sup>3</sup> H. Hosono, and Y. Abe, Inorg. Chem. **26**, 1192 (1987).  
<sup>4</sup> B. J. Ingram, and T. O. Mason, J. Electrochem. Soc. **150**, E396 (2003).  
<sup>5</sup> P. V. Sushko, A. L. Shluger, K. Hayashi, M. Hirano, and H. Hosono, Phys. Rev. Lett. **91**, 126401 (2003).  
<sup>6</sup> H. Bartl, and T. Scheller, Neues Jb. Miner. Mh. **35**, 547 (1970); A. N. Christensen, Acta Chem. Scand. **Ser. A** **41**, 110 (1987).  
<sup>7</sup> J. A. Imlach, L. S. D. Glasser, and F. P. Glasser, Cement Conc. Res. **1**, 57 (1971).  
<sup>8</sup> E. Wimmer, H. Krakauer, M. Weinert, and A. J. Freeman, Phys. Rev. B **24**, 864 (1981).  
<sup>9</sup> V. P. Dravid (unpublished).

- <sup>10</sup> For all H-bearing structures, the positions of H ions inside the cages were optimized using the DMol method; see, B. Delley, J. Chem. Phys. **113**, 7756 (2000).  
<sup>11</sup> Solutions of the effective one-electron equations are obtained by means of the linear muffin-tin orbital method in the atomic sphere approximation<sup>23</sup>. The band structure calculations were performed for the cell of  $12CaO \cdot 7Al_2O_3$  with one formula unit, i.e. a total of 59 atoms per cell which combine into six cages. In addition, 85 empty spheres were included to fill out the open space of the system.  
<sup>12</sup> For the investigations of the UV-irradiated mayenite, we used the virtual crystal approximation which accounts properly for the band-filling effects.  
<sup>13</sup> That mayenite falls into the fit of Fig. 4b in Ref. 2 and, hence, into the  $F^+$  center category, appears fortuitous. Our *ab-initio* investigations show that the absorption band energy of the  $F^+$  center in relaxed CaO depends strongly on tetragonal distortion: for the *same average* cation-anion distance, a tetragonal distortion of 1% (and 2%) results in an energy deviation of 2% (and 6%). In mayenite, the distortion is 25%; therefore, the energy deviation will be much larger. Thus, the use of an *average* cation-anion distance for mayenite<sup>2</sup> in the Mollwo-Ivey law is incorrect.  
<sup>14</sup> N. F. Mott, and E. A. Davis, *Electronic Processes in Non-crystalline Materials*, (Oxford Univ. Press, Oxford, 1979).  
<sup>15</sup> B. I. Shklovskii, and A. L. Efros, *Electronic Properties of Doped Semiconductors* (Springer-Verlag, Berlin, Heidelberg, 1984).  
<sup>16</sup> H. Böttger, and V. V. Bryksin, *Hopping Conduction in Solids* (Akademie-Verlag, Berlin, 1985); N. Van Lien, and R. Rosenbaum, J. Phys. Cond. Mat. **10**, 6083 (1998); A. G. Zabrodskii, Phil. Mag. B **81**, 1131 (2001).  
<sup>17</sup> M. Pollak, and M. L. Knotek, J. Non-crystal. Solids **32**, 141 (1979).  
<sup>18</sup> M. Sarvestani, M. Schreiber, and T. Vojta, Phys. Rev. B **52**, R3820 (1995).  
<sup>19</sup> N. F. Mott, *Conduction in Non-Crystalline Materials*, p. 28 (Clarendon Press, Oxford, 1987).  
<sup>20</sup> G. I. Zhmoidin, and G. S. Smirnov, Inorg. Mater. **18**, 1595 (1982).  
<sup>21</sup> M. Miyakawa, K. Hayashi, M. Hirano, Y. Toda, T. Kamiya, and H. Hosono, Adv. Mater. **15**, 1100 (2003).  
<sup>22</sup> M. Pollak, Phys. Stat. Sol. (b) **230**, 295 (2002).  
<sup>23</sup> O. K. Andersen, O. Jepsen, M. Sob, *Electronic Band Structure and its Applications*, (ed. M. Yussouff. Springer-Verlag, Berlin, 1986).

TABLE I. The relative contributions per atom to the DOS at  $E_F$ . Similar percentages are obtained from the integrated DOS in the energy range of  $E_F \pm 0.025$  eV.

Atoms	%	Atoms	%	Atom	%
Ca(1)	7.6	Ca(4)	4.2	rest Ca	$\sim 1.0$
Ca(2)	8.4	H*	6.9	rest O	$\sim 0.7$
O*	8.3	Centers of		Al	0.1
Ca(3)	3.8	empty cages	0.3		